International Journal of Thermophysics, Vol. 7, No. 2, 1986

Equilibrium and Nonequilibrium Computer Simulation Studies of Polar Fluids and Nonpolar Mixtures[1]

A. L. Kielpinski,[2] K. Mansour,[2] and S. Murad[2]

We present a technique for estimating intermolecular potential model parameters for polar compounds. This technique has been used for two polar compounds, hydrogen chloride and ammonia. The potential models are then used to study a wide range of static and dynamic properties using computer simulations. Where possible, results have been compared with experimental data to demonstrate the adequacy of the models. Static properties have been calculated using the methods of Monte Carlo and equilibrium molecular dynamics. The shear viscosity has been obtained using the nonequilibrium molecular dynamics method. Finally, we also report results for a computer simulation study of quadrupolar mixtures. This study investigates the changes in properties caused by a change in the sign of the quadrupole moment of one mixture component.

KEY WORDS: ammonia; hydrogen chloride; quadrupolar mixtures; molecular dynamics; Monte Carlo method.

1. INTRODUCTION

We report results of computer simulation studies of fluid hydrogen chloride and ammonia. These compounds were chosen as representative linear and nonlinear polar compounds, which are small enough in size so that assumption of molecular rigidity is quite accurate. However, despite this, both molecules have strong orientation-dependent forces and moderate

[1] Paper presented at the Ninth Symposium on Thermophysical Properties, June 24–27, 1985, Boulder, Colorado, U.S.A.

[2] Department of Chemical Engineering, University of Illinois at Chicago, Box 4348, Chicago, Illinois 60680, U.S.A.

0195-928X/86/0300-0421$05.00/0

polarizability [1], so that the effect of such forces on bulk and molecular properties can be investigated. Results are also reported for a study of model quadrupolar fluid mixtures. This study was undertaken to investigate the effect of the sign of the quadrupole moment on thermodynamic and transport properties.

Computer simulations for pure fluids were carried out using both the molecular dynamics (MD) and the Monte Carlo (MC) methods [2]. The results for static properties for both the techniques were the same to within their expected accuracy, so that we do not differentiate between these two methods. The properties studied included thermodynamic properties, structure, mean squared force and torque, dielectric constant, self-diffusion coefficient, and shear viscosity. These properties were calculated along the saturation curve for the pure fluids. Wherever possible the calculated results have been compared with experimental data. For the model mixtures, two dense fluid conditions were studied for each of two cases: (i) when both molecules in an equimolar mixture have similar quadrupoles and (ii) when the quadrupoles have opposite signs. Theory and experiment suggest that such mixtures should behave differently [3].

2. INTERMOLECULAR POTENTIALS

The intermolecular potential models for hydrogen chloride, ammonia, and the model fluids were all of the form

$$u(\mathbf{r}\omega_1\omega_2) = u(12) = u_0(12) + u_{\mu\mu}(12) + u_{\mu Q}(12) + u_{QQ}(12) + u_{\text{ind}}(12) \tag{1}$$

where $\mathbf{r}$ is the vector joining the centers of mass of molecules 1 and 2, ω_i is the orientation of molecule i, $u_0(12)$ is the central nonpolar potential, which we chose as the L – J (12, 6) potential,

$$u_0(12) = 4\varepsilon[(\sigma/r)^{12} - (\sigma/r)^6] \tag{2}$$

$u_{\mu\mu}$, $u_{\mu Q}$, and u_{QQ} are the contributions due to the permanent multipoles, while u_{ind} is the contribution due to polizability. This contribution is obtained via an iterative procedure as described by us in detail previously [4].

For the two model quadrupolar mixtures, the quadrupole moment for the components were all of the same magnitude, i.e., $|Q^*| = 1.0$; component B of the mixture of unlike-signed quadrupoles had $Q^* = -1.0$. The polarizability for all mixture components was $\alpha^* = 0.06$. For both hydrogen chloride and ammonia, the dipole and quadrupole moments were kept fixed at their experimental values, as was the dipole polarizability. This

Table I. Intermolecular Potential Models for Hydrogen Chloride and Ammonia

	Hydrogen chloride	Ammonia
ε/k (K)	270	203
σ (Å)	3.70	3.40
μ (esu · cm)	1.09×10^{-18}	1.47×10^{-18}
Q (esu · cm^2)	3.80×10^{-26}	-3.307×10^{-26} [20]
α (cm^3)	26.0×10^{-25}	22.6×10^{-25}

leaves the two L – J constants as parameters which were obtained using the technique described below.

The best parameters were first obtained by a simulataneous least-squares fit of the experimental and calculated second virial coefficient and dimer structure. The models thus obtained were then tested for the crystal lattice structure. For hydrogen chloride we found that the model gave a

Table II. Dimer and Crystal Lattice Structures and Energies for Hydrogen Chloride and Ammonia

Dimer structure and energy

	Hydrogen chloride		Ammonia	
	Calc.	Exp. or QM [4]	Calc.	Exp. or QM [16]
θ_1 (deg)	−9	−3 to −13	80	67
θ_2 (deg)	82	75 to 83	−11.	0
ϕ_{12} (deg)	0	0	0	0
r_{12} (Å)	3.76	3.81 to 3.95	3.32	3.05 to 3.53
$-E_{\text{dimer}}$ (kJ · mol^{-1})	8.92	7.00 to 9.00	11.82	8.37 to 18.83

Crystal lattice structure and energy

	Hydrogen chloride		Ammonia	
	Calc.	Exp. [4]	Calc.	Exp. or QM [17]
a (Å)	5.13	5.05	5.105	5.084
b (Å)	5.59	5.37	5.105	5.084
c (Å)	5.66	5.82	5.105	5.084
ρ (g · cm^{-3})	1.49	1.53	0.850	0.861–0.922
$-E$ (kJ · mol^{-1})	27.80	25.85	31.36	28.43–41.81

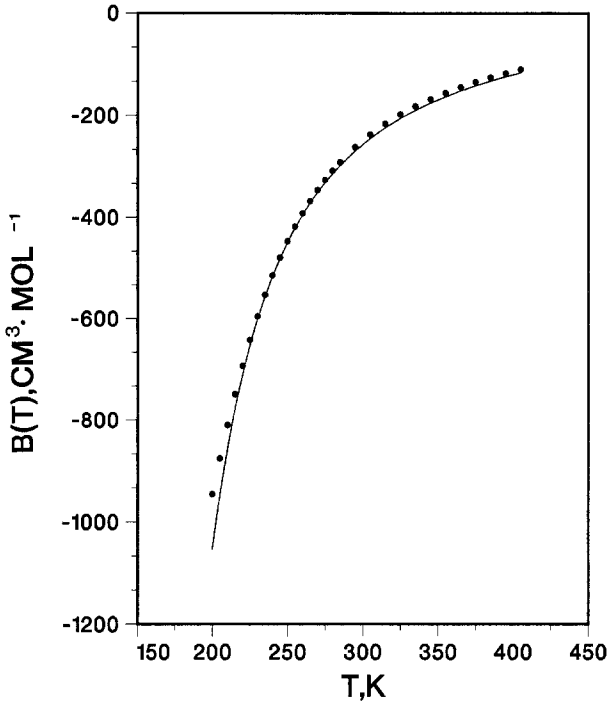

Fig. 1. Second virial coefficient $B(T)$ for ammonia from the potential model (——) and experiment [14] (···).

satisfactory ordered solid structure. For ammonia it was less satisfactory. The parameters were then adjusted slightly, to give a more reasonable solid structure, while maintaining good agreement for the virial and dimer. The potential models thus obtained for hydrogen chloride and ammonia are shown in Table I. The dimer and crystal lattice structures are shown in Table II, while the second virial coefficient of ammonia is shown in Fig. 1. A similar good agreement for the second virial coefficient was obtained for hydrogen chloride [4].

3. THE SIMULATION METHODS

Two types of molecular dynamics simulations were used. For all properties except shear viscosity we used equilibrium molecular dynamics using the quaternion algorithm [5] which we have described previously [4, 5]. The shear viscosity was obtained using a nonequilibrium molecular dynamics algorithm with homogeneous shear and time varying non-orthogonal boundary conditions [6]. The time steps for hydrogen chloride

and ammonia were 0.5×10^{-15} and 1.83×10^{-16} s, respectively, while for the model mixtures the dimensionless time step, $\Delta t^* = (\varepsilon/m)^{1/2} \sigma^{-1} \Delta t$, was 0.0003. In equilibrium simulations, 750 steps were allowed for equilibration, while in the nonequilibrium simulations, the velocity profile was constrained to be linear for the first 500 steps (which were not included in calculating any results). The equilibrium and nonequilibrium results are based on between 3000 and 7500 time steps, depending on the magnitude of fluctuations.

The Monte Carlo simulations were carried out using the conventional Metropolis algorithm for polyatomic systems [7]. The results reported are based on between 500,000 and 750,000 configurations, an initial 125,000 configurations being rejected for equilibration. The translational displacements were made by randomly moving a molecule within a cube of side 0.02 Å. The orientational displacements were made with a maximum angle shift of 0.0942 radian. This scheme led to an acceptance ratio of 50 to 80%.

For both MC and MD, the system consisted of 256 molecules. The potential was cut off at 3σ for the polar fluids and at 3.5σ for the model mixtures. Because both hydrogen chloride and ammonia have both large dipole and large quadrupole moments, long-range effects are expected to be small because of the different angle dependence of the various dipole–quadrupole interactions [8, 9]. Previous simulations have been reported for both hydrogen chloride [9] and ammonia [10]. Where possible we have compared results with previous simulations. We would like to add that none of the previous models has explicitly included polarizability, which is expected to make significant contributions to the properties of both hydrogen chloride and ammonia.

4. RESULTS

Figures 2–4 show some results for the properties of saturated liquid hydrogen chloride. Figure 2 shows the site–site correlation functions for a density of 22.9 mol·l^{-1} compared with experimental data of Soper and Egelstaff [11] and with a previous computer simulation [9]. Figure 3 shows results for the dielectric constant compared with experimental data. Finally, Fig. 4 shows results for the shear viscosity obtained using the nonequilibrium molecular dynamics method. The results show that the intermolecular potential model we have developed for hydrogen chloride is quite satisfactory and works well for a diverse group of properties. The potential also gives good results for the structure factor, self-diffusion coefficient, mean-squared torque, etc. These and some other properties will be reported in a separate communication [12].

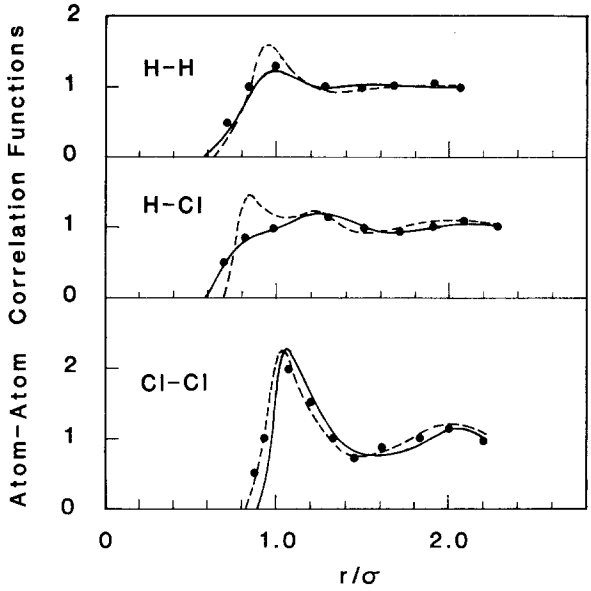

Fig. 2. Atom–atom correlation functions of saturated hydrogen chloride at 13.8×10^{27} molecules $\cdot$ m^{-3}: experiment [11] (···); potential model without polarizability [9] (---); potential model used in this study (——).

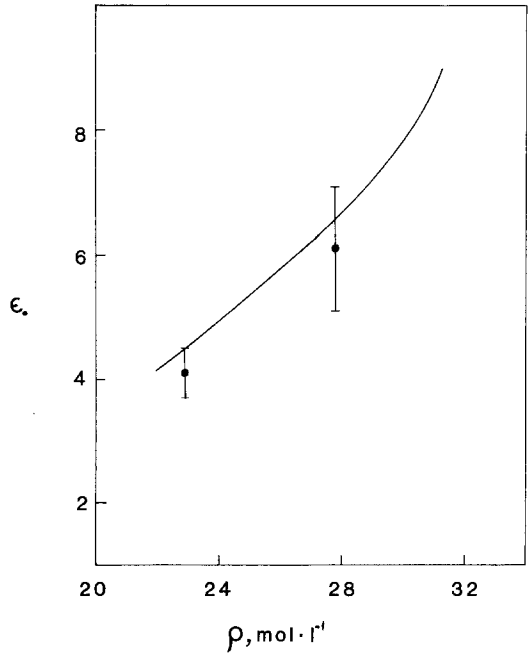

Fig. 3. Dielectric constant ε_0 for hydrogen chloride: experiment [18] (——); results of simulations (···).

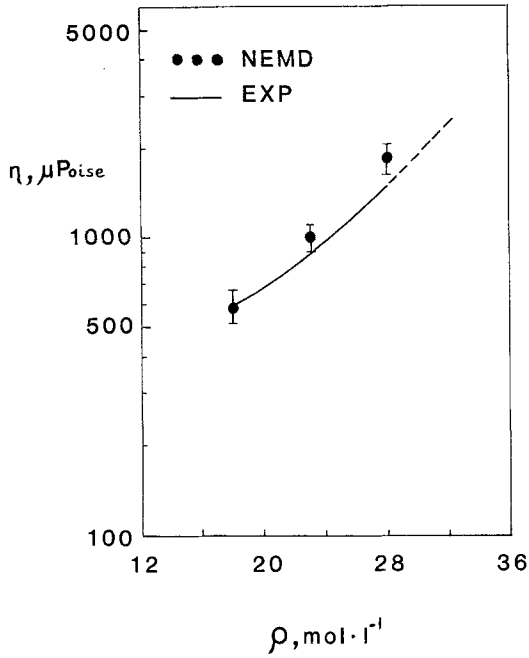

Fig. 4. Viscosity of hydrogen chloride: experiment [19] (——); results of NEMD simulations (···).

Figure 5 shows results for the site–site correlation function $g_{NN}(r)$ for ammonia, compared with experimental results of Narten [13] and other recent simulation results [10]. In Fig. 5 we have shown the most accurate models for $g_{NN}(r)$ compared with our results. We should mention here that these models in general do not necessarily give accurate results for the second virial coefficient and the dimer and crystal structure, as our model does. Nevertheless, our results are comparable to the best previous models. For this density the simulation gives values of $-18.07\,\mathrm{kJ \cdot mol^{-1}}$ and 1.06 for the internal energy and compressibility factor. Experimental values are $-19.92\,\mathrm{kJ \cdot mol^{-1}}$ and approximately 0, respectively. The pressures are not in good agreement. However, this is not unusual for computer simulations [10] for ammonia.

Finally, we show results for two types of equimolar homonuclear quadrupolar mixtures. The first mixture ($Q_A^* Q_B^* > 0$) had quadrupole moments of the same sign (positive) and strength ($Q^* = 1.0$), e.g., an isotopic mixture. The second mixture ($Q_A^* Q_B^* < 0$) had quadrupole moments of opposite sign but of the same strength (± 1.0). Figure 6 shows results for the various correlation functions of these two mixtures at

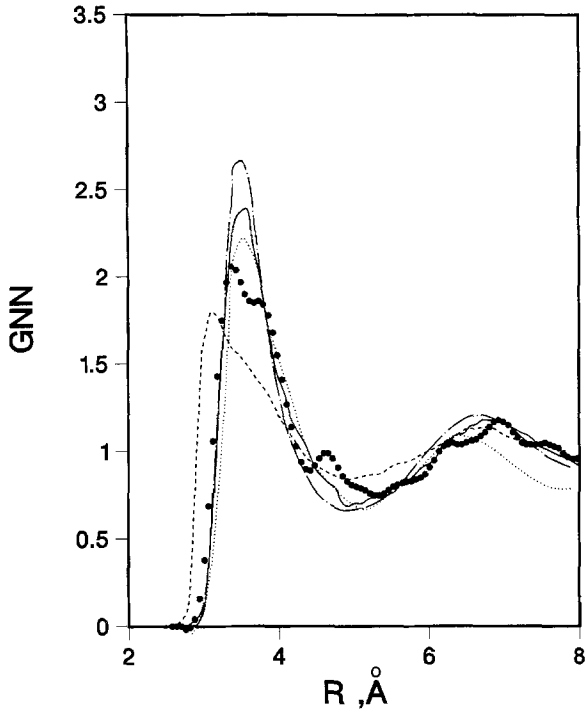

Fig. 5. Atom–atom correlation function $g_{NN}(r)$ for saturated NH_3 at 2.24×10^{28} molecules $\cdot$ m^{-3}: experiment [13] (· · ·); this study (——); previous simulation [10a] (– – –); previous simulation [10c] (Model A) (· · · · · · · · ·); previous simulation [10c] (Model B) (——————).

Table III. Thermodynamic Properties of Quadrupolar Mixtures

	$\rho^* = 0.4$		$\rho^* = 0.7$	
	$Q_A^* Q_B^* > 0$	$Q_A^* Q_B^* < 0$	$Q_A^* Q_B^* > 0$	$Q_A^* Q_B^* < 0$
$\langle T^* \rangle$	1.55	1.56	1.48	1.51
$\langle P/\rho kT \rangle$	0.21	0.21	0.60	0.52
$\langle u^* \rangle$	−3.48	−3.67	−6.12	−6.56
$\langle (\tau_A^*)^2 \rangle$	21.5	25.8	38.7	47.2
$\langle (\tau_B^*)^2 \rangle$	21.3	26.1	40.2	47.5
$\langle (F_A^*)^2 \rangle$	718	762	1363	1594
$\langle (F_B^*)^2 \rangle$	678	760	1385	1582
$\mu_{res,A}^*$	−1.81	−1.82	−2.05	−1.90
$\mu_{res,B}^*$	−1.81	−1.79	−2.05	−2.10

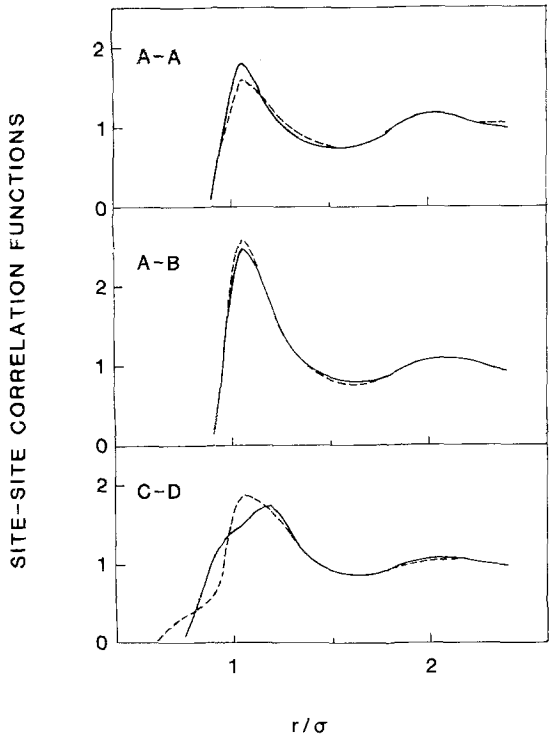

Fig. 6. Atom–atom correlation functions for quadrupolar mixtures at $\rho^* = 0.7$: $Q_A^* Q_B^* > 0$ (——); $Q_{AB}^{**} < 0$ (– – – – –).

$\rho^* = 0.7$. The COM of the two molecules are A and B respectively, while C and D represent the atoms of the two molecules. Results for other thermodynamic properties are as shown in Table III. As seen in Fig. 6 and Table III, the difference in quadrupole sign has a significant effect on the properties of dense fluid mixtures. At lower densities, the effects are less pronounced. It appears that the change in the sign of the quadrupole has the largest effect on the energy, mean-squared torque, and chemical potential. We plan to compare our results with perturbation theory methods to see if they will show similar differences. The residual chemical potential, $\mu_{res}^* \equiv (\mu - \mu_0)/kT$, was obtained using the fictitious test particle method of Widom [15].

5. CONCLUSIONS

We have presented a technique for developing accurate effective intermolecular potential models for polar compounds. The technique has been

tested for a range of static and dynamic properties, to demonstrate its adequacy.

The effect of the sign of the quadrupole moment on the properties of dense fluids has also been investigated. Our results show that the sign makes a significant contribution to both thermodynamic and structural properties.

REFERENCES

1. C. G. Gray and K. E. Gubbins, *Theory of Molecular Fluids. I* (Clarendon, Oxford, 1984).
2. W. B. Streett and K. E. Gubbins, *Ann. Rev. Phys. Chem.* **28**:373 (1977).
3. S. I. Sandler, *Mol. Phys.* **28**:107 (1974).
4. S. Murad, *Mol. Phys.* **51**:525 (1984).
5. D. J. Evans and S. Murad, *Mol. Phys.* **34**:327 (1977).
6. D. J. Evans, *Physica* **118A**:51 (1983).
7. P. A. Monson and K. E. Gubbins, *J. Phys. Chem.* **87**:2852 (1983).
8. G. N. Patey, D. Levesque, and J. J. Weis, *Mol. Phys.* **38**:1635 (1979).
9. S. Murad, K. E. Gubbins, and J. G. Powles, *Mol. Phys.* **40**:253 (1980); M. L. Klein and I. R. McDonald, *Mol. Phys.* **42**:243 (1981); D. Levesque, J. J. Weis, and D. W. Oxtoby, *J. Chem. Phys.* **79**:917 (1983); C. Votava, R. Ahlrichs, and A. Geiger, *J. Chem. Phys.* **78**:6841 (1983).
10. (a) W. L. Jorgensen and M. Ibrahim, *J. Am. Chem. Soc.* **102**:3309 (1980); (b) R. H. Kincaid and H. A. Scheraga, *J. Phys. Chem.* **86**:833 (1982); (c) A. Hinchliffe, D. G. Bounds, M. L. Klein, I. R. McDonald, and R. Righini, *J. Chem. Phys.* **74**:1211 (1981).
11. A. K. Soper and P. A. Egelstaff, *Mol. Phys.* **42**:399 (1981).
12. S. Murad, A. Papaioannou, and J. G. Powles, *Mol. Phys.* **56**:431 (1985).
13. A. H. Narten, *J. Chem. Phys.* **66**:3117 (1977).
14. L. Haar and J. S. Gallagher, *J. Phys. Chem. Ref. Data* **7**:635 (1978).
15. B. Widom, *J. Chem. Phys.* **39**:2808 (1963); J. G. Powles, *Mol Phys.* **41**:715 (1980).
16. J. D. Dill, L. C. Allen, W. C. Topp, and J. A. Pople, *J. Am. Chem. Soc.* **97**:7220 (1975); G. Brink and L. Glasser, *J. Comput. Chem.* **2**:177 (1981).
17. I. Olosson and D. H. Templeton, *Acta. Cryst.* **12**:832 (1959); R. A. Nemenoff, J. Snir, and H. A. Sheraga, *J. Phys. Chem.* **82**:2504 (1978); M. L. Klein, I. R. McDonald, and R. Righini, *J. Chem. Phys.* **7**:3673 (1979).
18. W. Harder, Ph. D. thesis (Karlsruhe, 1972); G. Glocker and R. E. Peck, *J. Chem. Phys.* **4**:658 (1936).
19. K. Krynicki and J. W. Hennel, *Acta Phys. Pol.* **24**:269 (1963).
20. S. G. Kukolich, *Chem. Phys. Lett.* **5**:401 (1970); *Chem. Phys. Lett.* **12**:216 (1971).